ActiveTwig: Morphology-Guided Active Reconstruction for Slender Structures Using Gaussian Splatting

***Abstract*— Accurate 3D reconstruction of slender branches is critical for robotic pruning, yet thin and occluded geometries challenge existing active perception systems. Current Gaussian Splatting (GS)-based methods typically rely on isotropic confidence metrics, leading to inefficient viewpoint allocation for tubular structures. We propose ActiveTwig, a morphology-guided active reconstruction framework that incorporates geometric anisotropy into viewpoint evaluation. By extracting the principal axis from GS primitives, we introduce a direction-aware confidence model that prioritizes circumferential observations. This is integrated into a target-centric Next-Best-View (NBV) strategy with ROI-constrained sampling and depth-aware weighting. Simulation results on TreeNet3D show that ActiveTwig improves skeleton accuracy by 17–27% and achieves up to 100% success rate in topology completion, outperforming GS-based and coverage-driven baselines.**

I. Introduction

High-throughput phenotyping is essential for precision agriculture, supporting downstream tasks such as robotic pruning and yield estimation [1]–[5]. Accurately digitizing tree architecture requires robust 3D reconstruction and precise branch segmentation [6]–[8]. However, the complex and highly occluded structure of dormant trees renders static sensing insufficient [9]. Active perception, through sequential Next-Best-View (NBV) planning, is therefore required to resolve occlusions and recover complete morphology [10]. To bridge perception development and field deployment, a staged paradigm is necessary, where controlled simulation or laboratory settings—e.g., using a robotic manipulator—enable isolation of core perceptual challenges before scaling to mobile platforms [11]–[13].

Classical discretized representations (e.g., occupancy grids) fail to capture the geometric continuity required for branch-level analysis [14]–[16]. Recent Radiance-Field-based approaches, particularly Gaussian Splatting (GS) [17], enable efficient high-fidelity reconstruction and have been adopted in active mapping pipelines [18]–[20]. However, existing GS-based planners typically rely on isotropic confidence or Fisher information metrics [21]–[24], neglecting the directional anisotropy of tubular structures, where observations orthogonal to the branch axis are more informative than longitudinal views [25], [26].

We propose ActiveTwig, a morphology-guided active perception framework that exploits primitive-level geometric anisotropy within the GS representation. By introducing a direction-aware confidence metric, ActiveTwig prioritizes informative viewpoints and improves efficient branch topology completion in dense canopies. We validate the framework in simulation and controlled robotic settings, establishing a robust baseline for scalable robotic phenotyping.

II. Methodology

ActiveTwig is a morphology-guided active perception framework for object-centric reconstruction of slender structures. As illustrated in Fig. 1, the system follows a perception–mapping–evaluation–planning pipeline. We maintain a hybrid environment representation that combines a coarse voxel map $\mathcal{V}$ for collision-aware navigation and a 2DGS map $\mathcal{G}$ for high-fidelity geometric modeling. The 2DGS representation models the scene using surface-aligned Gaussian primitives, capturing local surface orientation and geometry. This property is particularly suitable for slender structures such as branches, where accurate surface alignment provides strong directional cues. Building on this representation, the key component of our framework is an anisotropy-aware viewpoint evaluation module that leverages these directional cues to guide NBV selection, favoring observations that maximize structural information in thin and occluded regions while suppressing redundant views along the structure direction.

1) Morphology-guided anisotropic confidence: Existing GS-based active mapping methods (e.g., ActiveGS [23]) typically assume isotropic surface geometry, leading to inefficient viewpoint allocation for elongated structures such as branches. In contrast, ActiveTwig exploits the intrinsic anisotropy encoded in 2DGS primitives. Each Gaussian is surface-aligned and captures local geometric orientation, from which we estimate a principal direction $\mathbf{u}_i$.

As shown in Fig. 1 (center), we evaluate candidate viewpoints based on their angular relationship to this direction. Specifically, we define an anisotropic utility as

$$U_{\text{aniso}}(v_i) \propto 1 - |\mathbf{v}_i \cdot \mathbf{u}_i| \,, \tag{1}$$

where $\mathbf{v}_i$ denotes the viewing direction. This formulation favors observations orthogonal to the structure, which provide stronger geometric constraints, while suppressing redundant longitudinal views. This directional preference is incorporated into viewpoint utility estimation, enabling the planner to actively select views that maximize structural information gain, particularly in heavily occluded regions.

2) Target-aware object-centric planning: To improve efficiency in unbounded canopy environments, we constrain candidate viewpoints within a target-centric Region-of-Interest (ROI), as illustrated in Fig. 1. This prevents the robot from drifting into irrelevant free space while maintaining focus on the object of interest. In addition, we introduce a depth-aware exploitation strategy that prioritizes near-field observations, which are particularly beneficial for refining

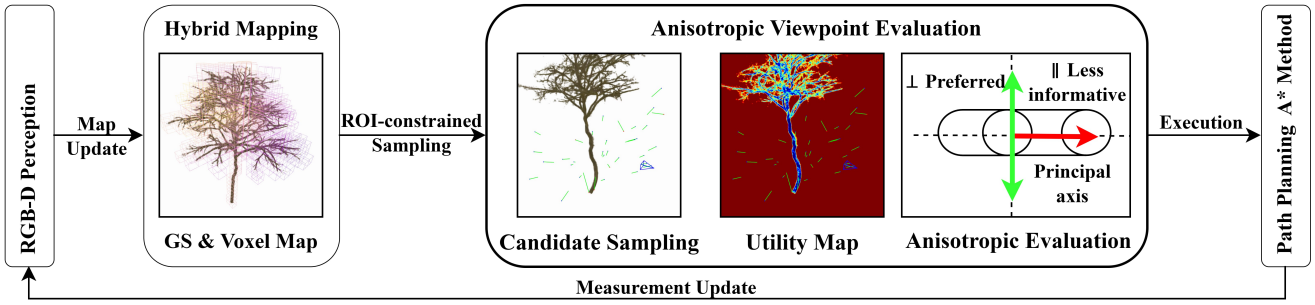

Fig. 1: Overview of ActiveTwig. RGB-D measurements update a hybrid GS–voxel map. Anisotropic viewpoint evaluation guides exploration, and selected views are executed via path planning to close the perception–action loop.

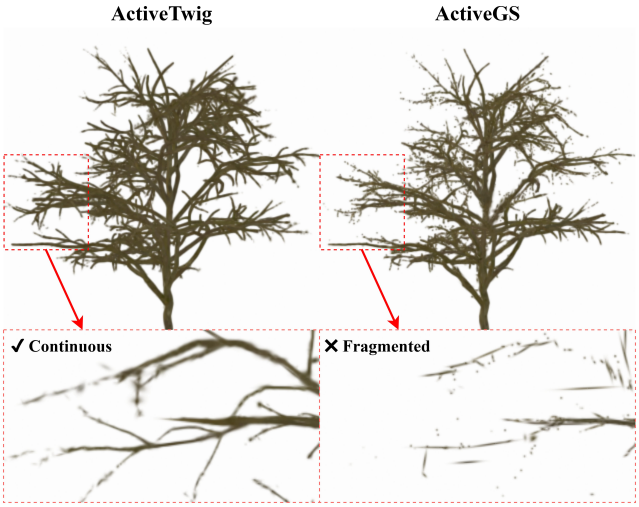

Fig. 2: ActiveTwig (left) vs. ActiveGS (right). Anisotropy-aware NBV improves branch continuity in occluded regions.

the fine-scale geometry of thin structures. The final NBV is selected by balancing volumetric exploration and anisotropic geometry refinement, where exploration encourages coverage and anisotropic evaluation promotes informative viewpoints aligned with local structure. Collision-free trajectories are computed using voxel-based planning on $\mathcal{V}$, ensuring safe and efficient viewpoint execution.

3) Extensibility towards structure-aware perception: Beyond geometric reconstruction, the proposed representation supports structure-aware reasoning for downstream tasks such as phenotyping and robotic pruning. In particular, the reconstructed 2DGS map can be extended to branch-level segmentation, enabling the extraction of meaningful structural components from complex canopy scenes. While segmentation is not explicitly modeled in the current pipeline, the improved geometric fidelity provided by anisotropic active perception facilitates more reliable and consistent structure extraction. This design allows ActiveTwig to serve as a robust perception backbone that can be readily integrated with higher-level task modules in future robotic systems.

III. Experiments and Results

We evaluate ActiveTwig in simulation on two tree types (Lemon and Cherry) using the Habitat simulator [27] and TreeNet3D dataset [28]. We compare against ActiveGS [23], along with FBE [29] and ablated variants.

1) Reconstruction quality: As shown in Fig. 2 (Lemon), ActiveTwig produces more continuous and complete branch structures, while ActiveGS exhibits fragmented reconstructions in occluded regions. Quantitatively, our method reduces Skeleton Chamfer Distance by up to 27% and improves F-score by 10%, indicating more accurate recovery of thin structures. Similar trends are observed on other tree types.

2) Exploration efficiency: ActiveTwig reaches the predefined completeness threshold 40.7% faster than FBE, demonstrating more efficient viewpoint allocation. This improvement is primarily attributed to ROI-constrained sampling, which avoids unnecessary exploration of free space.

3) Robustness and ablation: ActiveTwig achieves a 98%–100% success rate across 100 Monte Carlo trials, significantly outperforming ActiveGS, which often fails due to early exploration drift. Ablation studies further confirm that ROI filtering is essential for stable exploration, while anisotropic confidence and depth-awareness contribute to improved reconstruction of slender structures.

IV. Conclusion

We presented ActiveTwig, a morphology-guided active perception framework for object-centric reconstruction of slender structures. By incorporating geometric anisotropy from 2DGS primitives into viewpoint evaluation, ActiveTwig enables direction-aware planning that prioritizes structurally informative observations. ActiveTwig achieves more continuous and complete branch reconstruction, while existing GS-based methods suffer from fragmented structures in occluded regions. Our method reduces skeleton reconstruction error by up to 27% and achieves near-perfect success rates, demonstrating improved efficiency and robustness. These results show that coupling representation geometry with planning is critical for efficient reconstruction of thin structures in unbounded environments.

REFERENCES

[1] A. Jain, C. Grimm, and S. Lee, "Learning to prune branches in modern tree-fruit orchards," in *2025 IEEE International Conference on Robotics and Automation (ICRA)*. IEEE, 2025, pp. 15 553–15 559.

[2] G. Liu, B. Boom, N. Slob, Y. Durodié, A. Nowé, and B. Vanderborght, "Automated behavior planning for fruit tree pruning via redundant robot manipulators: Addressing the behavior planning challenge," pp. 2–12. [Online]. Available: https://ieeexplore.ieee.org/document/10978028/

[3] A. Atefi, Y. Ge, S. Pitla, and J. Schnable, "Robotic technologies for high-throughput plant phenotyping: Contemporary reviews and future perspectives," *Frontiers in plant science*, vol. 12, p. 611940, 2021.

[4] R. Xu and C. Li, "A review of high-throughput field phenotyping systems: Focusing on ground robots," *Plant phenomics*, 2022.

[5] Y. Huang, Z. Ren, D. Li, and X. Liu, "Phenotypic techniques and applications in fruit trees: a review," *Plant Methods*, vol. 16, no. 1, p. 107, 2020.

[6] Y. Fu, Y. Xia, H. Zhang, M. Fu, Y. Wang, W. Fu, and C. Shen, "Skeleton extraction and pruning point identification of jujube tree for dormant pruning using space colonization algorithm," *Frontiers in Plant Science*, vol. 13, p. 1103794, 2023.

[7] Y. Li, Z. Zhang, X. Wang, W. Fu, and J. Li, "Automatic reconstruction and modeling of dormant jujube trees using three-view image constraints for intelligent pruning applications," *Computers and Electronics in Agriculture*, vol. 212, p. 108149, 2023.

[8] X. Bu, C. Liu, H. Liu, G. Yang, Y. Shen, and J. Xu, "Dfsnet: A 3d point cloud segmentation network toward trees detection in an orchard scene," *Sensors*, vol. 24, no. 7, p. 2244, 2024.

[9] H. R. Sankaramaddi, W. S. Lee, K. Kim, and Y. Hong, "2d-to-3d image reconstruction in agriculture: A review of methods, challenges, and ai-driven opportunities," *Sensors*, vol. 26, no. 6, p. 1775, 2026.

[10] R. Bajcsy, "Active perception," *Proceedings of the IEEE*, vol. 76, no. 8, pp. 966–1005, 1988.

[11] T. Qiu, A. Zoubi, L. Cheng, and Y. Jiang, "3d branch point cloud completion for robotic pruning in apple orchards," *arXiv preprint arXiv:2404.05953*, 2024.

[12] A. K. Burusa, J. Scholten, X. Wang, D. Rapado-Rincón, E. J. van Henten, and G. Kootstra, "Semantics-aware next-best-view planning for efficient search and detection of task-relevant plant parts," *Biosystems Engineering*, vol. 248, pp. 1–14, 2024.

[13] A. Navone, M. Martini, and M. Chiaberge, "Autonomous robotic pruning in orchards and vineyards: A review," *Smart Agricultural Technology*, p. 101283, 2025.

[14] J. I. Vasquez-Gomez, L. E. Sucar, R. Murrieta-Cid, and E. Lopez-Damian, "Volumetric next-best-view planning for 3d object reconstruction with positioning error," *International Journal of Advanced Robotic Systems*, vol. 11, no. 10, p. 159, 2014.

[15] R. Zeng, W. Zhao, and Y.-J. Liu, "Pc-nbv: A point cloud based deep network for efficient next best view planning," in *2020 IEEE/RSJ International Conference on Intelligent Robots and Systems (IROS)*. IEEE, 2020, pp. 7050–7057.

[16] A. Hornung, K. M. Wurm, M. Bennewitz, C. Stachniss, and W. Burgard, "Octomap: An efficient probabilistic 3d mapping framework based on octrees," *Autonomous robots*, vol. 34, no. 3, pp. 189–206, 2013.

[17] B. Kerbl, G. Kopanas, T. Leimkühler, G. Drettakis *et al.*, "3d gaussian splatting for real-time radiance field rendering." *ACM Trans. Graph.*, vol. 42, no. 4, pp. 139–1, 2023.

[18] S. Zhu, G. Wang, X. Kong, D. Kong, and H. Wang, "3d gaussian splatting in robotics: A survey." [Online]. Available: http://arxiv.org/abs/2410.12262

[19] R. Jin, Y. Gao, Y. Wang, Y. Wu, H. Lu, C. Xu, and F. Gao, "GS-planner: A gaussian-splatting-based planning framework for active high-fidelity reconstruction," in *2024 IEEE/RSJ International Conference on Intelligent Robots and Systems (IROS)*. IEEE, pp. 11 202–11 209. [Online]. Available: https://ieeexplore.ieee.org/document/10801715/

[20] Z. Xu, R. Jin, K. Wu, Y. Zhao, Z. Zhang, J. Zhao, F. Gao, Z. Gan, and W. Ding, "HGS-planner: Hierarchical planning framework for active scene reconstruction using 3d gaussian splatting," in *2025 IEEE International Conference on Robotics and Automation (ICRA)*. IEEE, pp. 14 161–14 167. [Online]. Available: https://ieeexplore.ieee.org/document/11127649/

[21] W. Jiang, B. Lei, and K. Daniilidis, "Fisherrf: Active view selection and mapping with radiance fields using fisher information," in *European Conference on Computer Vision*. Springer, 2024, pp. 422–440.

[22] Y. Xie, Y. Cai, Y. Zhang, L. Yang, and J. Pan, "GauSS-MI: Gaussian splatting shannon mutual information for active 3d reconstruction." [Online]. Available: http://arxiv.org/abs/2504.21067

[23] L. Jin, X. Zhong, Y. Pan, J. Behley, C. Stachniss, and M. Popović, "ActiveGS: Active scene reconstruction using gaussian splatting," vol. 10, no. 5, pp. 4866–4873. [Online]. Available: https://ieeexplore.ieee.org/document/10938898/

[24] Y. Li, Z. Kuang, T. Li, Q. Hao, Z. Yan, G. Zhou, and S. Zhang, "ActiveSplat: High-fidelity scene reconstruction through active gaussian splatting," vol. 10, no. 8, pp. 8099–8106. [Online]. Available: https://ieeexplore.ieee.org/document/11037548/

[25] M. Vázquez-Arellano, H. W. Griepentrog, D. Reiser, and D. S. Paraforos, "3-d imaging systems for agricultural applications—a review," *Sensors*, vol. 16, no. 5, p. 618, 2016.

[26] E. Marchand and F. Chaumette, "Active vision for complete scene reconstruction and exploration," *IEEE Transactions on Pattern Analysis and Machine Intelligence*, vol. 21, no. 1, pp. 65–72, 2002.

[27] X. Puig, E. Undersander, A. Szot, M. D. Cote, R. Partsey, J. Yang, R. Desai, A. W. Clegg, M. Hlavac, T. Min, T. Gervet, V. Vondrus, V.-P. Berges, J. Turner, O. Maksymets, Z. Kira, M. Kalakrishnan, J. Malik, D. S. Chaplot, U. Jain, D. Batra, A. Rai, and R. Mottaghi, "Habitat 3.0: A co-habitat for humans, avatars and robots," 2023.

[28] S. Tang, Z. Ao, Y. Li, H. Huang, L. Xie, R. Wang, W. Wang, and R. Guo, "TreeNet3d : A large scale tree benchmark for 3d tree modeling, carbon storage estimation and tree segmentation," vol. 130, p. 103903. [Online]. Available: https://linkinghub.elsevier.com/retrieve/pii/S1569843224002577

[29] B. Yamauchi, "A frontier-based approach for autonomous exploration," in *Proceedings 1997 IEEE International Symposium on Computational Intelligence in Robotics and Automation CIRA'97.'Towards New Computational Principles for Robotics and Automation'*. IEEE, 1997, pp. 146–151.